# Chemical Models of Cytochrome P450 Catalyzed Insecticide Metabolism. Application to the Oxidative Metabolism of Carbamate Insecticides

György M. Keserü,*,[†] György Balogh,[†] Irén Czudor,[†] Tamás Karancsi,[‡] András Fehér,[†] and Béla Bertók[†]

Department of Chemical Research, CHINOIN AGCHEM Business Unit, P.O. Box 49,
H-1780 Budapest, Hungary, and Central Research Institute of Chemistry, Hungarian Academy of Sciences,
P.O. Box 21, H-1521 Budapest, Hungary

Cytochrome P450 (CP450) catalyzed oxidative metabolism of carbofuran (**1**), carbaryl (**2**), and pirimicarb (**3**) has been modeled using biomimetic oxidations catalyzed by iron(III) tetraarylporphyrins. Oxidation products of **1** were identified by comparison of HPLC retention times measured under standardized conditions for metabolites synthesized and characterized by $^1$H and $^{13}$C NMR spectroscopy. Comparison of product distributions to in vivo metabolic profiles revealed that the $H_2O_2$/*meso*-tetrakis(pentafluorophenyl)porphyrin iron(III) chloride [Fe(TF$_{20}$PP)] system mimics the action of insect CP450s against carbofuran. The effectiveness of this system was further demonstrated by the biomimetic oxidation of other carbamate insecticides (**2** and **3**) monitored by HPLC/electrospray MS. The predictive power of this biomimetic model was compared to that of knowledge-based expert systems. Although similar models were recently applied in pharmaceutical research, the usefulness of this approach has first been demonstrated for the prediction of metabolic profiles of agrochemicals.

**Keywords:** *Oxidative metabolism; cytochrome P450; biomimetic oxidation; iron(III) tetraarylporphyrins; carbamate insecticides; metabolite synthesis; HPLC/electrospray MS*

## INTRODUCTION

Cytochrome P450 (CP450) is one of the most important systems responsible for the oxidative metabolism of insecticides (Hodgson et al., 1993). Increased activity of this enzyme has been linked to the development of metabolic resistance against formerly active agrochemicals (Feyereisen, 1995; Mulin and Scott, 1992). The first observation of the involvement of P450 in the resistance to pesticides was reported by Eldefrawi et al. (1960), who counteracted carbaryl resistance with the methylenedioxyphenyl P450 inhibitor, Sesamex. Studies on carbamate-selected houseflies also revealed that resistant strains possessed increased hydroxylation, dealkylation, and epoxidation potencies relative to susceptible strains (Hassal, 1990). Resistance management techniques involve the application of new active ingredients, special formulations, or genetically immunized crops. In addition to these methods, it has been recognized that the synergistic action of selective metabolic inhibitors might be also beneficial to decrease resistance (Lamoureux and Rusness, 1995).

Development of metabolic inhibitors requires an extensive knowledge of the molecular mechanism of CP450-catalyzed oxidative reactions. Due to the complexity of reactions catalyzed by P450 mono-oxygenases, modeling studies are recognized as an important tool for the understanding of molecular mechanisms of these metabolic processes. Simultaneous action of different isoforms observed in vivo and in vitro provides a macroscopic view to the system, whereas structural and theoretical biochemistry, as well as bioorganic chemistry, enables an insight at the molecular level. Theoretical investigations of CP450-catalyzed insecticide metabolism have recently been published from our laboratory (Keserü et al., 1997; Keserü, 1998).

Synthetic metalloporphyrins (Montanari and Casella, 1994) were found to be useful as chemical mimics of peroxidases, whereas the peroxide shunt observed in the catalytic cycle of CP450 represents a similar transformation that can also be modeled using synthetic metalloporphyrins. Although several biomimetic transformations for drugs have been successfully performed using these catalysts (Andersen et al., 1994; Nagatsu et al., 1990), agrochemical applications of synthetic metalloporphyrins have been rather limited. To the best of our knowledge, modeling of the oxidative metabolism of carbamate insecticides is the first example.

In this work, we studied the biomimetic oxidation of carbamate insecticides to find answers to the following questions: (1) Can chemical models be used to mimic the CP450-catalyzed oxidative metabolism of carbamate insecticides? (2) Can metabolically sensitive functional groups be identified in this way? (3) Do these model systems adequately reproduce experimental metabolic profiles? To clarify the above problems, metalloporphyrin-catalyzed oxidations of carbofuran (**1**), carbaryl (**2**), and pirimicarb (**3**) in the presence of several co-oxidants were carried out.

* Author to whom correspondence should be addressed (fax +36-1-4241200; e-mail gykeseru@goliat.eik.bme.hu).
† CHINOIN AGCHEM Business Unit.
‡ Hungarian Academy of Sciences.

Chemical Models for CP450

*J. Agric. Food Chem.,* Vol. 47, No. 2, 1999 **763**

## EXPERIMENTAL PROCEDURES

$^1$H and $^{13}$C NMR spectra were obtained by a Bruker AC-200 spectrometer in CDCl$_3$ using tetramethylsilane as an internal standard. IR spectra were recorded on a Perkin-Elmer 398 spectrometer. UV absorption spectra were recorded on a Shimadzu UV-160 spectrometer. Reverse-phase HPLC was used to obtain purity data and retention times for all metabolites of **1**. These analyses were performed using a Hewlett-Packard 1050 system equipped with a Spherisorb 5 ODS-1 column. An acetonitrile/water (40:60) gradient was used with photometric detection at 220 nm by setting the flow rate to 1 mL/min. Metabolite profiles of **2** and **3** were obtained by HPLC/MS measurements. An HPLC system equipped with a Symmetry C8 (Waters) 3.9 × 150 column, a Spectraphysics P200 gradient pump, a UV100 detector, and a 10 µL Rheodyne injector was used for these analyses using the eluent system of eluent A (acetonitrile/water/formic acid, 5:95:0.1) and eluent B (acetonitrile/water/formic acid, 95:5:0.1) in a gradient of 100% A to 100% B in 20 min. Metabolites were photometrically detected at 254 nm by setting the flow rate to 1 mL/min. Mass spectrometry studies were performed by a VG QUATTRO triplequad spectrometer (Micromass, Manchester, U.K.) with electrospray ionization. An electrospray source temperature of 120 °C, a cone voltage of 15 V, and an eluent split of 1:10 were applied. Scan parameters were set to scan over a range of $m/z$ 10–100 in 1 min. Centroid data were acquired.

Merck Kieselgel F254 TLC plates were used for the monitoring of reactions.

**Chemicals.** All reagents as well as *meso*-tetrakis(pentafluorophenyl)porphyrin iron(III) chloride [Fe(TF$_{20}$PP)] were obtained from Aldrich Chemical Co. (Milwaukee, WI). Solvents were of analytical grade and purchased from Chemolab Ltd. (Hungary).

**7-Hydroxy-2,2-dimethyl-2,3-dihydrobenzofuran (4).** Carbofuran (**1**) was hydrolyzed according to the procedure of Balba et al. (1968) (3.31 g, 15 mmol) using alcoholic potassium hydroxide (1.01 g, 18 mmol) to give **4** (1.85 g, 77%): bp 70 °C (80 Pa);$^1$H NMR δ 1.50 (s, 6H, 2 × CH$_3$), 3.05 (s, 2H, CH$_2$), 5.19 (br s, 1H, OH), 6.73 (s, 3H, Ar); $^{13}$C NMR δ 28.52 (2 × CH$_3$), 43.92 (C-3), 88.21 (C-2), 114.83 (C-4), 116.91 (C-5), 120.91 (C-6), 127.92 (C-7a), 140.23 (C-7), 146.12 (C-3a); IR $\nu_{max}$ 3567, 1625, 1606, 1479, 1300, 1253 cm$^{-1}$ (CHCl$_3$); TLC [eluent, benzene/diethyl ether (1:3)] $R_f$ 0.63; HPLC retention time (min) $t_R$ 6.86. Anal. Calcd for C$_{10}$H$_{12}$O$_2$: C, 73.14; H, 7.37. Found: C, 72.84; H, 7.83.

**Benzyloxymethylcarbamic Acid 2,2-Dimethyl-2,3-dihydrobenzofuran-7-yl Ester (5).** To a solution of 0.82 g (5 mmol) of **4** in dry benzene (25 mL) and triethylamine (0.1 mL) was added 0.82 g (5 mmol) of benzyloxymethyl isocyanate. The mixture was refluxed for 18 h and then extracted with diethyl ether. The organic phase was dried over MgSO$_4$ and evaporated to yield **5** as a colorless solid (1.05 g, 66%): mp 60–62 °C; $^1$H NMR δ 1.49 (s, 6H, 2 × CH$_3$), 3.05 (s, 2H, CH$_2$), 4.66 (s, 2H, OCH$_2$), 4.85 (d, 2H, NCH$_2$), 5.97 (t, 1H, NH), 6.77, 7.42 (m, 8H, Ar); $^{13}$C NMR δ 28.13 (2 × CH$_3$), 43.07 (C-3), 70.26 (NCH$_2$), 72.02 (BzCH$_2$), 88.34 (C-2), 120.11, 121.61, 122.39, 127.74, 127.95, 128.42, 129.54, 137.82 (C–Ar), 134.50 (C-7a), 150.18 (C-3a), 153.34 (CO); IR $\nu_{max}$ 3443, 1752, 1482, 1231, 1136 cm$^{-1}$ (CHCl$_3$). Anal. Calcd for C$_{19}$H$_{21}$NO$_4$: C, 69.70; H, 6.43; N, 4.27. Found: C, 69.56; H, 6.32; N, 4.15.

**Hydroxymethylcarbamic Acid 2,2-Dimethyl-2,3-dihydrobenzofuran-7-yl Ester (6).** To a solution of 0.32 g (1 mmol) of **5** with CCl$_4$ (20 mL) was added 1 g (5 mmol) of trimethylsilyl iodide, and the reaction mixture was stirred for 1 h and filtered. The filtrate was quenched with MeOH (4-fold excess) and stirred overnight. The solvent was then evaporated and the residue dissolved in diethyl ether, extracted with aqueous sodium bisulfite, aqueous sodium bicarbonate, and aqueous NaCl and dried over MgSO$_4$. Evaporation yielded 0.14 g (50%) of **6** as colorless crystals: mp 133–135 °C; $^1$H NMR δ 1.50 (s, 6H, 2 × CH$_3$), 3.04 (s, 2H, CH$_2$), 3.41 (s, 1H, OH), 4.35 (d, 2H, NCH$_2$), 5.38 (s, 1H, NH), 6.74–7.37 (m, 3H, Ar);$^{13}$C NMR δ 22.92 (2 × CH$_3$), 43.86 (C-3), 73.61 (CH$_2$OH), 89.08 (C-2), 120.91 (C-4), 121.83 (C-5), 121.91 (C-

6), 127.92, (C-7a), 130.72 (C-7), 137.95 (C-3a); IR $\nu_{max}$ 3345, 1730, 1225, 1131 cm$^{-1}$ (KBr); TLC (diethyl ether/hexane, 2:1) $R_f$ 0.54; HPLC retention time (min) $t_R$ 3.15. Anal. Calcd for C$_{12}$H$_{15}$NO$_4$: C, 60.74; H, 6.32; N, 5.90. Found: C, 61.21; H, 6.23; N, 5.81.

**2,2-Dimethyl-7-methylcarbamoyloxybenzofuran-3-one (7).** A solution of **1** (4.4 g, 20 mmol) in acetic acid (20 mL) was oxidized with chromium trioxide (12.16 g, 80 mmol) at 25–30 °C for 16 h with continuous stirring. The reaction mixture was then quenched with water (30 mL) and extracted with diethyl ether. Evaporation of the solvent gave **7** (3.00 g, 65%) as colorless crystals: mp 163–165 °C (ethanol);$^1$H NMR δ 1.48 (s, 6H, 2 × CH$_3$), 2.92 (d, 3H, NCH$_3$), 5.19 (s, 1H, NH), 7.00–7.54 (m, 3H, Ar); $^{13}$C NMR δ 22.99 (2 × CH$_3$), 27.90 (NCH$_3$), 89.08 (C-2), 121.64 (C-4), 121.79 (C-5), 131.03 (C-6), 123.57 (C-7a), 137.26 (C-7), 153.90 (C-3a), 161.12 (CO), 204.33 [(C-3)O]; IR $\nu_{max}$ 3358, 1717, 1620, 1500, 1271 cm$^{-1}$(KBr); TLC (diethyl ether/benzene, 3:1) $R_f$ 0.27; HPLC retention time (min) $t_R$ 5.51. Anal. Calcd for C$_{12}$H$_{15}$NO$_4$: C, 61.27; H, 5.57; N, 5.95. Found: C, 60.8; H, 5.2; N, 6.1.

**3,7-Dihydroxy-2,2-dimethylbenzofuran (8).** To a solution of **5** (0.3 g 1.2 mmol) in dry methanol was added 0.094 g (2.5 mmol) of sodium borohydride. After the total conversion of the starting material, the reaction mixture was evaporated and the residue chromatographed using silica gel 60 [eluent, diethyl ether/benzene (3:1)] to give **8** (0.08 g, 40%) as a colorless oil: $^1$H NMR δ 1.35 (s, 3H, CH$_3$), 1.49 (d, 3H, CH$_3$), 2.11 (d, 1H, COH), 4.76 (d, 1H, CH), 5.75 (s, 1H, ArOH), 6.75, 6.98 (m, 3H, Ar); $^{13}$C NMR δ 20.84 (2 × CH$_3$), 79.04 (C-2), 90.66 [(C-3)OH], 117.00 (C-4), 117.72 (C-5), 121.59 (C-6), 128.33 (C-7a), 140.91 (C-7), 146.12 (C-3a); TLC (diethyl ether/benzene, 3:1) $R_f$ 0.49; HPLC retention time (min) $t_R$ 3.46. Anal. Calcd for C$_{10}$H$_{12}$O$_3$: C, 67.11; H, 5.66. Found: C, 66.96; H, 5.51.

**Methylcarbamic Acid 2,2-Dimethyl-3-hydroxy-2,3-dihydrobenzofuran-7-yl Ester (9).** To a solution of **7** (0.47 g, 2 mmol) in methanol (10 mL) was added sodium cyanoborohydride (0.16 g, 2.5 mmol). pH was maintained between 3.1 and 3.4 using 5 N aqueous HCl at 45 °C for 3 h. The reaction mixture was then quenched with water (5 mL), filtered, and extracted with diethyl ether. The ether extract was dried over MgSO$_4$, and the solvent was evaporated. The residue was chromatographed on silica gel 60 using diethyl ether/benzene (3:1) as gradient. **9** was obtained as colorless crystals (0.16 g, 35%): mp 105–108 °C; $^1$H NMR δ 1.34 (s, 3H, CH$_3$), 1.48 (s, 3H, CH$_3$), 2.52 (d, 1H, OH), 2.87 (d, 3H, NCH$_3$), 4.71 (d, 1H, CH), 5.08 (s, 1H, NH), 6.83, 7.25 (m, 3H, Ar); $^{13}$C NMR δ 20.74 (2 × CH$_3$), 26.17 (NCH$_3$), 78.54 (C-2), 90.84 [(C-3)OH], 120.79 (C-4), 123.84 (C-5), 124.08 (C-6), 130.87 (C-7a), 135.26 (C-7), 150.90 (C-3a), 154.52 (CO); IR $\nu_{max}$ 3574, 1718, 1295, 1124, 910 cm$^{-1}$ (CHCl$_3$); TLC [eluent, benzene/methanol (5:1)] $R_f$ 0.43; HPLC retention time (min) $t_R$ 3.7. Anal. Calcd for C$_{12}$H$_{15}$NO$_4$: C, 60.74; H, 6.36; N, 5.90. Found: C, 60.9; H, 6.1; N, 5.7.

**7-Hydroxy-2,2-dimethylbenzofuran-3-one (10).** Carbamate **7** (3.52 g, 15 mmol) was hydrolyzed with alcoholic potassium hydroxide (1.01 g, 18 mmol in 40 mL of ethanol) at 40–45 °C for 2 h. The reaction mixture was acidified using 5 N aqueous HCl and extracted with diethyl ether. The extract was then dried over MgSO$_4$, and the solvent was evaporated to give **10** (2.55 g, 96%) as colorless crystals: mp 162–165 °C; $^1$H NMR δ 1.49 (s, 6H, 2 × CH$_3$), 5.86 (s, 1H, OH), 6.93, 7.36 (m, 3H, Ar); $^{13}$C NMR δ 23.10 (2 × CH$_3$), 89.15 (C-2), 116.20 (C-4), 120.37 (C-7a), 122.52 (C-5), 122.83 (C-6), 142.73 (C-7), 159.20 (C-3a), 204.33 [(C-3)O]; IR $\nu_{max}$ 3566, 1716, 1621, 1453, 1288, 1257, 1124, 918 cm$^{-1}$ (CHCl$_3$); TLC (diethyl ether/benzene, 3:1) $R_f$ 0.58; HPLC retention time (min) $t_R$ 4.62. Anal. Calcd for C$_{10}$H$_{10}$O$_3$: C, 67.41; H, 5.66. Found: C, 67.16; H, 5.51.

**Benzyloxymethylcarbamic Acid 2,2-Dimethyl-3-oxo-2,3-dihydrobenzofuran-7-yl Ester (11).** To a solution of **10** (0.89 g, 5 mmol) in dry benzene (25 mL) and triethylamine (0.1 mL) was added 0.82 g (5 mmol) of benzyloxymethyl isocyanate. The mixture was refluxed for 18 h and extracted with diethyl ether. The organic phase was dried over MgSO$_4$ and evaporated to yield **11** as a colorless solid (1.53 g, 90%):

mp 119−121 °C; $^1$H NMR $\delta$ 1.48 (s, 6H, 2 × CH$_3$), 4.67 (s, 2H, ArCH$_2$), 4.85 (d, 2H, NCH$_2$), 5.99 (s, 1H, NH), 6.02, 7.57 (m, 8H, Ar); $^{13}$C NMR $\delta$ 22.99 (2 × CH$_3$), 70.50 (NCH$_2$), 72.12 (BzCH$_2$), 89.21 (C-2), 121.83, 122.02, 122.39, 127.89, 128.52, 130.79, 137.58 (Ar), 136.93 (C-7a), 150.18 (C-3a), 153.64 [(C-3)O], 203.41 [(C-3)O]. Anal. Calcd for C$_{19}$H$_{19}$NO$_5$: C, 66.84; H, 5.56; N, 4.10. Found: C, 66.4; H, 5.3; N, 4.1.

**Hydroxymethylcarbamic Acid 2,2-Dimethyl-3-oxo-2,3-dihydrobenzofuran-7-yl Ester (12).** To a solution of 0.52 g (1.5 mmol) of **5** in CCl$_4$ (20 mL) was added trimethylsilyl iodide (1.5 g, 7.5 mmol), and the reaction mixture was stirred for 1 h and filtered. The filtrate was quenched with MeOH (4-fold excess) and stirred overnight under argon atmosphere. The solvent was then evaporated, and the residue was dissolved in diethyl ether, extracted with aqueous sodium bisulfite, aqueous sodium bicarbonate, and aqueous NaCl, and dried over MgSO$_4$. Evaporation of the solvent yielded 0.2 g (60%) **12** as colorless crystals: mp 141−145 °C; $^1$H NMR $\delta$ 1.48 (s, 6H, 2 × CH$_3$), 3.43 (s, 1H, OH), 4.75 (d, 2H, NCH$_2$), 5.98 (s, 1H, NH), 7.02, 7.57 (m, 3H, Ar);$^{13}$C NMR $\delta$ 22.95 (2 × CH$_3$), 73.91 (CH$_2$OH), 89.17 (C-2), 121.79 (C-4), 121.97 (C-5), 127.98 (C-6), 130.79 (C-7), 120.91 (C-7a), 137.85 (C-3a), 153.85 [(C-3)O], 204.16 [(C-3)O]; IR $\nu_{max}$ 3348, 1752, 1405, 1095 cm$^{-1}$ (CHCl$_3$); TLC [eluent, diethyl ether/benzene (3:1)] $R_f$ 0.47; HPLC retention time (min) $t_R$ 6.85. Anal. Calcd C$_{12}$H$_{13}$NO$_5$: C, 57.36; H, 5.17; N, 5.57. Found: C, 57.2; H, 5.2; N, 5.6.

***meso*-Tetrakis(2,6-dichlorophenyl)porphyrin Iron(III) Chloride [Fe(TCl$_8$PP)].** A solution of 2,6-dichlorobenzaldehyde (13.5 g, 77.1 mmol), pyrrole (5.35 mL, 77.1 mmol), and zinc acetate (5.35 g, 23.2 mmol) in 2,6-lutidine (116 mL) was placed in a 250 mL round-bottom flask equipped with a Soxhlet extractor. The extractor was filled with dried Na$_2$SO$_4$, and the reaction mixture was refluxed for 5 h. The solvent was evaporated, and the residue was dissolved in toluene and kept at 0 °C overnight. The purple precipitate was collected to give Zn(TCl$_8$PP) (14.88 g, 20%). The free porphyrin base was obtained by treating the solution of Zn(TCl$_8$PP) (1.86 g, 2 mmol) in dichloromethane (250 mL) with trifluoroacetic acid (19 mL) for 6 h at room temperature. The reaction mixture was extracted with aqueous NaHCO$_3$ and water, the organic layer was separated, and 50 mL of MeOH was added and evaporated. The residue was recrystallized from MeOH to give the free base (0.41 g, 24%), which was transformed to Fe(TCl$_8$-PP) by refluxing its solution in degassed DMF (270 mL) with FeCl$_2$·4H$_2$O (2.04 g, 2 mmol) for 4 h. Air was bubbled through the resulting brown solution for 10 h followed by evaporation. The residue was dissolved in 1 N HCl, and the dark brown participate was filtered off to yield Fe(TCl$_8$PP) (0.18 g, 57%). All intermediates and the product were identified by comparing their UV absorption spectra to literature data.
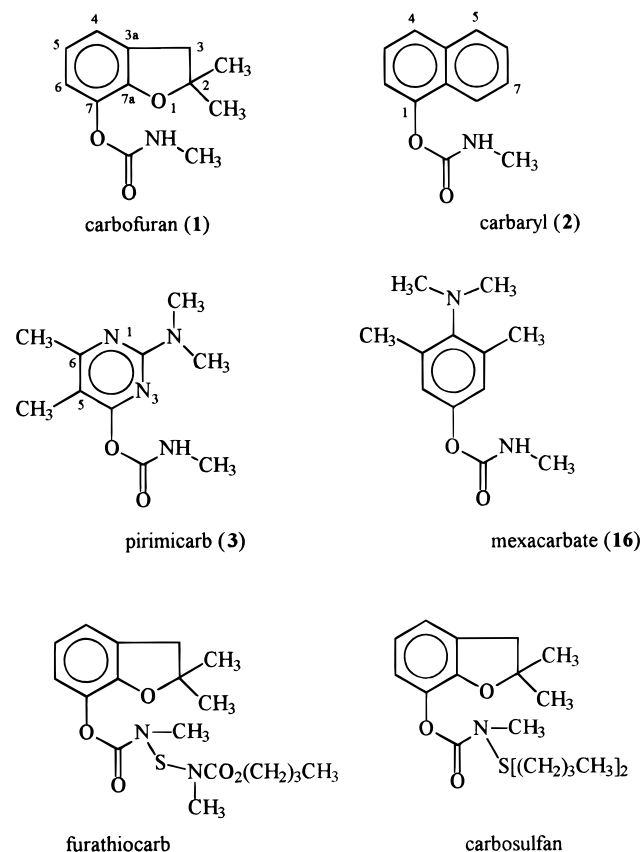
**General Procedure of Biomimetic Oxidations.** Carbamate insecticide (1.1 mmol) and 0.01 molar equiv of the catalyst were dissolved in 30 mL of the solvent, and 0.4 molar equiv of the oxidizing agent was added. The reaction mixture was stirred for 30 min at room temperature and the solvent evaporated. The residue was directly analyzed by HPLC. Oxidations effected by mCPBA were performed in dichloromethane; NaOCl and H$_2$O$_2$ were used in methanol/dichloroethane (1:1).

**Characterization of Metabolites Obtained by the Biomimetic Oxidation of Pirimicarb (3).** 5,6-Dimethyl-2-(methylformamido)-4-pyrimidinyl dimethylcarbamate (**15**) and 5,6-dimethyl-2-(methylamino)-4-pyrimidinyl dimethylcarbamate (**17**) were isolated from the mCPBA-mediated biomimetic oxidation of **3** catalyzed by Fe(TF$_{20}$PP). Preparative TLC [eluent, diethyl ether/benzene (3:1)] was used for the purification of samples identified by MS and $^1$H and $^{13}$C NMR spectroscopy.

***15***: MS (M + 1), 253; $^1$H NMR $\delta$ 2.12 (s, 3H, 5-CH$_3$), 2.47 (s, 3H, 6-CH$_3$), 3.05 and 3.11 [s, 3H, CON(CH$_3$)$_2$], 3.35 (s, 3H, NH−CH$_3$), 9.75 (s, 1H, CHO); $^{13}$C NMR $\delta$ 10.50 (5-CH$_3$), 22.43 (6-CH$_3$), 36.77 [CON(CH$_3$)$_2$], 115.00 (5-C), 152.80 [CON(CH$_3$)$_2$], 163.84 (NCHO), 164.22 (2-C), 168.87 (4-C), 178.15 (6-C).

***17***: MS (M + 1), 225; $^1$H NMR $\delta$ 2.04 (s, 3H, 5-CH$_3$), 2.34 (s, 3H, 6-CH$_3$), 2.93 (br d, 3H, NHCH$_3$), 3.04 and 3.12 [s, 3H,

**Chart 1**



carbofuran (**1**)

carbaryl (**2**)

pirimicarb (**3**)

mexacarbate (**16**)

furathiocarb

carbosulfan

CON(CH$_3$)$_2$], 7.37 (br m, 1H, NH−CH$_3$); $^{13}$C NMR $\delta$ 10.49 (5-CH$_3$), 22.44 (6-CH$_3$), 25.94 (CONHCH$_3$), 36.79 [N(CH$_3$)$_2$], 107.10 (5-C), 152.81 (CONHCH$_3$), 160.62 (2-C), 168.01 (4-C), 177.97 (6-C).

## RESULTS AND DISCUSSION

Oxidative metabolism of carbamate insecticides has been studied in plants, insects, and mammals (Kuhr and Dorough, 1976). In this study we selected the commercially most important carbamate insecticides, which are shown in Chart 1.

On the basis of radiolabeling studies, the major metabolite of carbofuran (**1**) was identified as 3-hydroxycarbofuran (**7**), along with *N*-hydroxymethyl (**6**) and 7-hydroxy analogues (**4**) as minor components (Metcalf et al., 1968). These compounds can be further transformed to the corresponding 3-keto (**7**), 3,7-dihydroxy (**8**), and 3-keto-7-hydroxy (**9**) metabolites before conjugation and excretion (Figures 1 and 2). Oxidative metabolites of carbaryl (**2**) were identified as the corresponding *N*-hydroxymethyl carbamate and metabolites hydroxylated at the aromatic ring (Figure 3) (Dorough and Casida, 1964; Knaak et al., 1965). Oxidative biotransformation of pirimicarb (**3**) involves demethylation of the dimethylamine moiety and oxidation of the methyl group at C-6 (Figure 4) (*The Pesticide Manual*, 1997).

Because the two other commercially most important carbamate insecticides, furathiocarb and carbosulfan (Chart 1), are also transformed to **1** along their detoxification pathway (*The Pesticide Manual*, 1997) oxidative metabolism of carbofuran is of outstanding importance. In addition to this, the huge amount of experimental data published on the metabolism of carbofuran also suggested that **1** be selected as the first test compound

Chemical Models for CP450

*J. Agric. Food Chem.,* Vol. 47, No. 2, 1999 **765**
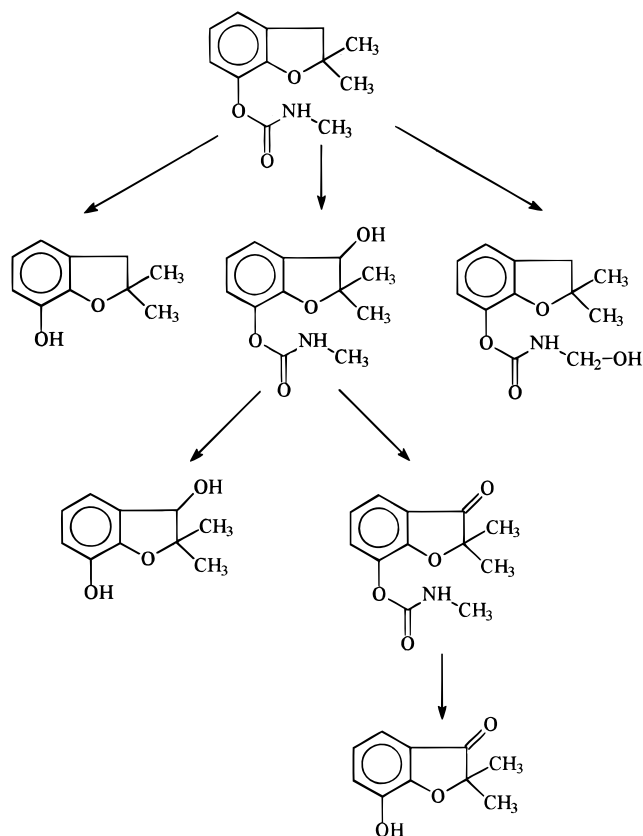


**Figure 1.** Metabolism of **1** in insects.

for the evaluation of our chemical models. An improved synthesis of carbofuran metabolites has been developed to obtain analytical standards for HPLC measurements.

**Synthesis of Carbofuran Metabolites.** The first synthesis of carbofuran metabolites has been reported by Balba et al. (1968). Our synthetic strategy is depicted in Figure 2. **4** was obtained by hydrolysis of **1** using alcoholic KOH and was transformed to **5** by reacting it with benzyloxyisocyanate (Balba et al., 1968). Removal of the benzyloxy protecting group was first carried out by hydrogenation using 10% Pd/C, which yielded only **13** corresponding to the cleavage of the N–CH$_2$ bond. Debenzylations effected by 5 N HCl or BF$_3$·Et$_2$O/EtSH (Fuji et al., 1979) also led to **13** selectively. Breaking the O–CH$_2$ bond was finally achieved by trimethylsilyl iodide (Jung and Lyster, 1977) to give **6**.

Metabolites **8**–**10** and **12** were prepared from 3-keto-carbofuran (**7**) obtained by the regioselective oxidation of **1** with chromium trioxide. Hydrolysis of **7** gave the 3-keto-7-hydroxy metabolite (**10**), which was transformed to **12** via the corresponding benzyloxy derivative **11** by treatment with trimethylsilyl iodide. In contrast to the original synthesis (Metcalf et al., 1968), the treatment of **1** with acetic acid gave the corresponding 3-acetoxycarbofuran in rather low yield. The major metabolite (**9**) was therefore synthesized from the 3-keto analogue (**7**) by reducing the carbonyl group with sodium cyanoborohydride under acidic conditions. Reduction of **7** with sodium borohydride resulted in the simultaneous hydrolysis of the carbamate side chain to give **8** as the major product. In conclusion, our improved strategy allowed the preparation of all 3-oxy metabolites from a single precursor. Metabolites were identified on the basis of their $^1$H and $^{13}$C NMR spectra and were analyzed by HPLC. HPLC retention times measured

under standardized conditions were used to identify products obtained from biomimetic oxidations of **1**.

**Biomimetic Oxidations.** Halogenated *meso*-tetra-arylporphyrins are known as efficient chemical models mimicking CP450-catalyzed oxidative transformations (Dolphin et al., 1997). It has been demonstrated by Dolphin et al. that *meso*-tetrakis(2,6-dichlorophenyl)-porphyrin iron(III) chloride [Fe(TCl$_8$PP)] is one of the most effective catalysts for biomimetic oxidations (Traylor et al., 1984). Fe(TCl$_8$PP) was therefore synthesized using an improved procedure recently published by Johnstone and Chorghade (Johnstone et al., 1996; Chorghade et al., 1996). The reactive ferryloxy intermediate was generated using a number of oxidizing agents such as alkyl peroxides, peracides, iodosylarenes, and inorganic oxidants (potassium peroxosulfate, sodium hypochlorite, hydrogen peroxide). Investigating the mechanism of alkyl peroxide mediated oxidations MacFaul et al. (1997) showed recently that it was the RO• radical rather than the iron(IV)oxy porphyrin which oxidized the substrate. Considering the high oxidation potential of iodosylarenes, these compounds are very likely to oxidize carbamates even in the absence of catalysts. Biomimetic oxidation of **1**–**3** was therefore carried out using *m*-chloroperbenzoic acid (mCPBA), sodium hypochlorite, and hydrogen peroxide in the presence of Fe(TCl$_8$PP). For **1**, reaction mixtures were analyzed by HPLC and oxidation products were identified using carbofuran metabolites as internal standards (Table 1). For **2** and **3**, reaction mixtures were injected to an HPLC/MS system and metabolites were identified on the basis of molecular ions and fragmentations. In the case of **3**, the structures of main metabolites were also verified by $^1$H and $^{13}$C NMR spectroscopy. Product distributions were calculated as a difference between oxidations performed with and without the catalyst. All reactions were repeated three to five times using the protocol described under Experimental Procedures. Data collected in the tables were calculated as the average of experiments. The error is ±0.5% of the reported value.

*Biomimetic Oxidation of **1**.* Comparing the results with the metabolite profile measured in houseflies (*Musca domestica*), we found that in contrast to in vivo experiments, hydrolysis of the carbamate side chain took place in all systems. In the case of NaOCl, due to the alkaline medium, this hydrolysis became dominant. In addition to the major metabolite **9**, oxidation at the C3 center yielded the 3-keto metabolite (**7**) as well. Oxidations associated with the simultaneous hydrolysis of the carbamate group led to the formation of products (**8** and **12**) derived by multistep transformations.

It has been recently reported that fluorinated metalloporphyrins are even more efficient and more selective catalysts in biomimetic oxidations (Chorghade et al., 1994). Oxidations catalyzed by the most popular *meso*-tetrakis(pentafluorophenyl)porphyrin iron(III) chloride [Fe(TF$_{20}$PP)] were therefore carried out to improve the performance of our model (Table 1). Use of mCPBA as oxidant resulted in the almost selective formation of **12**. Oxidations with H$_2$O$_2$, however, reproduced rather well the in vivo profile. Fair agreement between our model and the in vivo process is possibly due to the fact that in biological systems H$_2$O$_2$ could also substitute for NADPH and molecular oxygen in the catalytic cycle of P450s (the peroxide shunt). Increased resistance of Fe(TF$_{20}$PP) against oxidative degradation may be re-
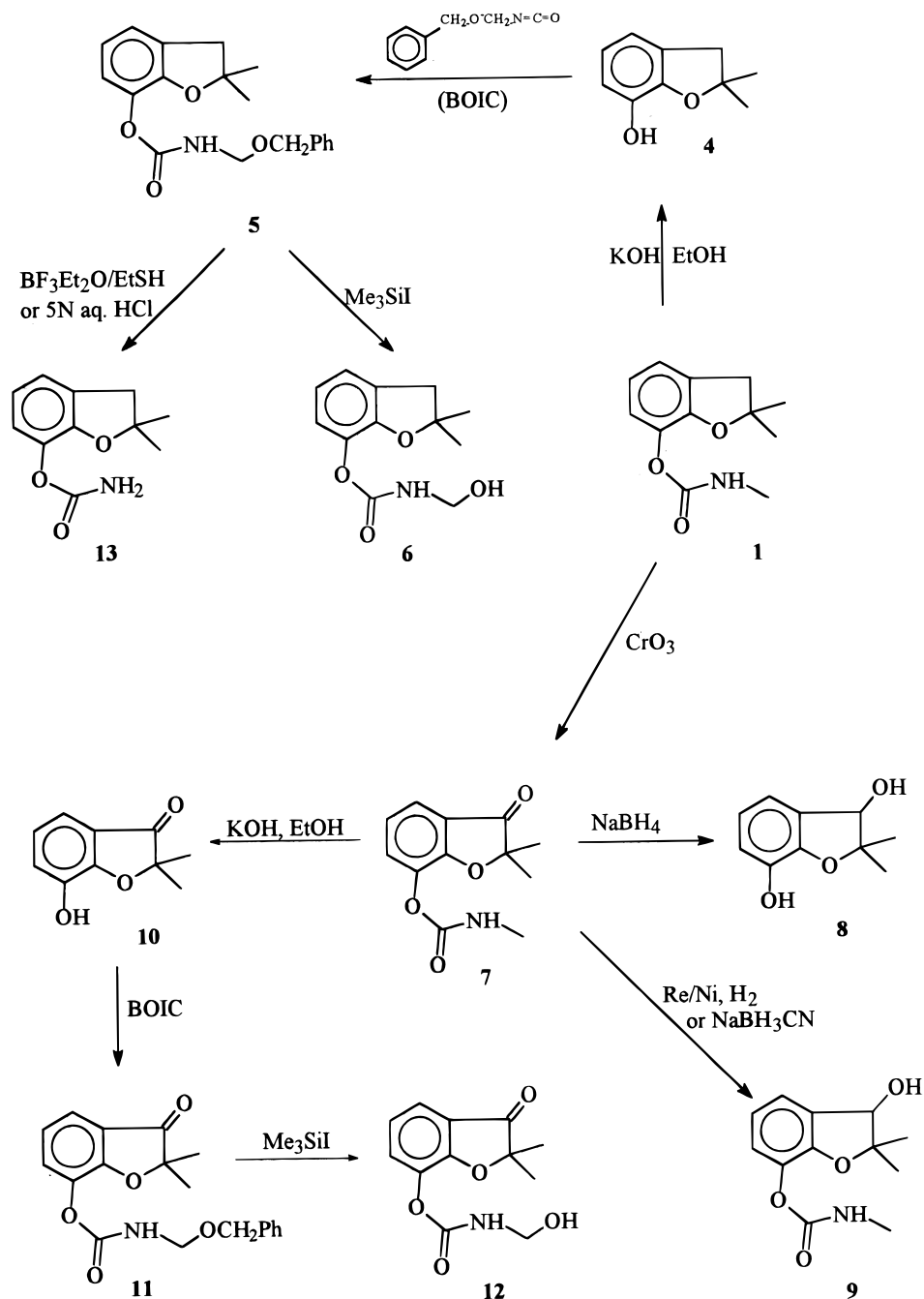
**Figure 2.** Synthesis of the oxidative metabolites of **1**.

sponsible for differences between product distributions observed in Fe(TCl₈PP)- and Fe(TF₂₀PP)-catalyzed reactions. The success achieved in the Fe(TF₂₀PP)-catalyzed biomimetic oxidation of **1** prompted us to use this catalyst for the oxidative transformation of **2** and **3** as well.

*Biomimetic Oxidation of **2**.* Fe(TF₂₀PP)-catalyzed oxidation of **2** was performed by $H_2O_2$ and mCPBA. Reactions performed in the presence of mCPBA gave only traces of oxidation products; however, monitoring $H_2O_2$-mediated reactions revealed the conversion of the starting material. Oxidation products were identified by direct comparison of TLC results [eluent, diethyl ether/hexane (4:1)] to that of the known metabolites (Dorough and Casida, 1964). In addition to the significant amount of **2**, the main product was identified as the corresponding *N*-hydroxycarbamate (**14**), whereas ring hydroxyl-

ated products were detected only in traces by MS (Figure 3). Comparing the in vivo metabolite profile to that obtained by the chemical model, it is apparent that ring hydroxylated metabolites (4-hydroxy, 5-hydroxy, and 5,6-dihydroxy) were produced only in trace by the biomimetic system. The limited rate of aromatic hydroxylations can be interpreted by the fact that in metalloporphyrin-catalyzed oxidations the aromatic moiety remains usually unchanged. Because only activated aromatics can undergo biomimetic oxidation (Artaud et al., 1993; Keserü et al., 1999), the reduced formation of ring hydroxylated product is a limitation of the model system with respect to enzymatic processes.

*Biomimetic Oxidation of **3**.* Product distributions detected in $H_2O_2$- and mCPBA-promoted oxidation of **3** catalyzed by Fe(TF₂₀PP) are presented in Table 2. Oxidation products were identified by HPLC/electro-
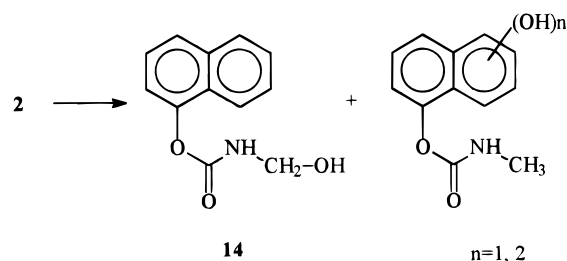
**Figure 3.** Products obtained by the biomimetic oxidation of **2**.

**Table 1. Product Distributions (Percent) Obtained by the Biomimetic Oxidation of 1[a]**

| $t_R$ | metab- olite | Fe(TCl$_8$PP) | | | Fe(TF$_{20}$PP) | | *M. domestica* in vivo |
|---|---|---|---|---|---|---|---|
| | | NaOCl | mCPBA | H$_2$O$_2$ | mCPBA | H$_2$O$_2$ | |
| 3.1 | **6** | 35.7 | 1.2 | – | – | 9.7 | 5.4 |
| 3.4 | **8** | 12.9 | 9.1 | 18.3 | – | – | – |
| 3.7 | **9** | 14.8 | 6.2 | 14.0 | 0.5 | 23.7 | 22.1 |
| 4.6 | **10** | – | 15.7 | 6.8 | 0.2 | – | – |
| 5.5 | **7** | – | – | – | – | 4.6 | 3.4 |
| 6.8 | **12** | 3.7 | – | – | 34.1 | 2.2 | – |
| 7.8 | **1** | 0.0 | 67.0 | 54.7 | 64.0 | 52.8 | 42.3 |

[a] All data are differences between product distributions obtained with and without the catalysts and were calculated as the average of three to five experiments. Dashes stand for compounds not detected.

spray MS, which was found to be useful in residue analysis (Volmer, 1998). In addition to its sensitivity and selectivity, electrospray ionization MS was found to be optimal for the analysis of oxidation products. Because degradation of these compunds might occur using CI and EI techniques, atmospheric pressure chemical ionization (APCI) was first applied. Degradation observed using this relatively soft ionization technique prompted us to use electrospray ionization for the MS analysis of reaction mixtures obtained by the biomimetic oxidation of **3**. Oxidations performed by the H$_2$O$_2$/Fe(TF$_{20}$PP) system yielded the corresponding *N*-formyl derivative (**15**) as the main component (Figure 4). In accordance with in vivo data, the dimethyl carbamate group was unchanged. Formation of **15** was rationalized by the oxidation of a methyl group at the amine moiety. Although **15** has not yet been isolated as a metabolite of **3**, similar *N*-formyl compounds were detected in the oxidative metabolism of mexacarbate

**Table 2. Product Distributions (Percent) Obtained by the Biomimetic Oxidation of 3[a]**

| | | oxidizing agent | |
|---|---|---|---|
| M + 1 | metabolite | mCPBA | H$_2$O$_2$ |
| 253 | **15** | 47.5 | 23.8 |
| 255 | **19** | 4.9 | – |
| 255 | **18** | 13.9 | – |
| 241 | **20** | 13.0 | – |
| 225 | **17** | 20.7 | – |
| 271 | **21** | – | 9.1 |
| 239 | **3** | – | 67.1 |

[a] Data were calculated as the average of three to five experiments. Dashes stand for compounds not detected.

(**16**) (Benezet and Matsumura, 1977), a carbamate insecticide substituted by a dimethylamino group at the aromatic ring. Oxidative metabolism of **16** leads to the corresponding N-demethylated analogue via the formation of this *N*-formyl intermediate. Identification of the *N*-formyl metabolite of **3** suggests this mechanism to be involved in the oxidative demethylation of the *N,N*-dimethylamino group of **3** in vivo. Our proposal was supported by the mCPBA/Fe(TF$_{20}$PP)-catalyzed oxidation of **3**. In addition to the previously described **15**, the corresponding N-demethylated compound (**17**) could also be detected. Because **15** and **17** are of crucial importance with respect to the metabolism of **3**, these compounds were isolated by preparative TLC and were identified by their $^1$H and $^{13}$C NMR spectra. In conclusion, we suggest that demethylation of the *N,N*-dimethyl moiety in **3** proceeds via **15**, which has not yet been detected in vivo. From a comparison of the structures of **3** and **16**, it is clear that the *N,N*-dimethyl group is the metabolically most sensitive function in **3**, whereas the monomethyl group at the carbamate nitrogen of **16** represents an alternative site for metabolic oxidation. The *N,N*-dimethyl group of **3** is therefore rapidly demethylated in vivo, which is indicated by the lack of **15** from the in vivo metabolite profile.

The formation of pyrimidine *N*-oxides (**18** and **19**) was also revealed by their characteristic MS fragmentation. This reaction was more characteristic in the presence of mCPBA, where the corresponding N-demethylated *N*-oxide (**19**) could also be isolated. Because mCPBA is known as an oxidizing agent used for the N-oxidation of heterocycles, the formation of *N*-oxides is not unexpected (Brown, 1994). Note, however, that the formation
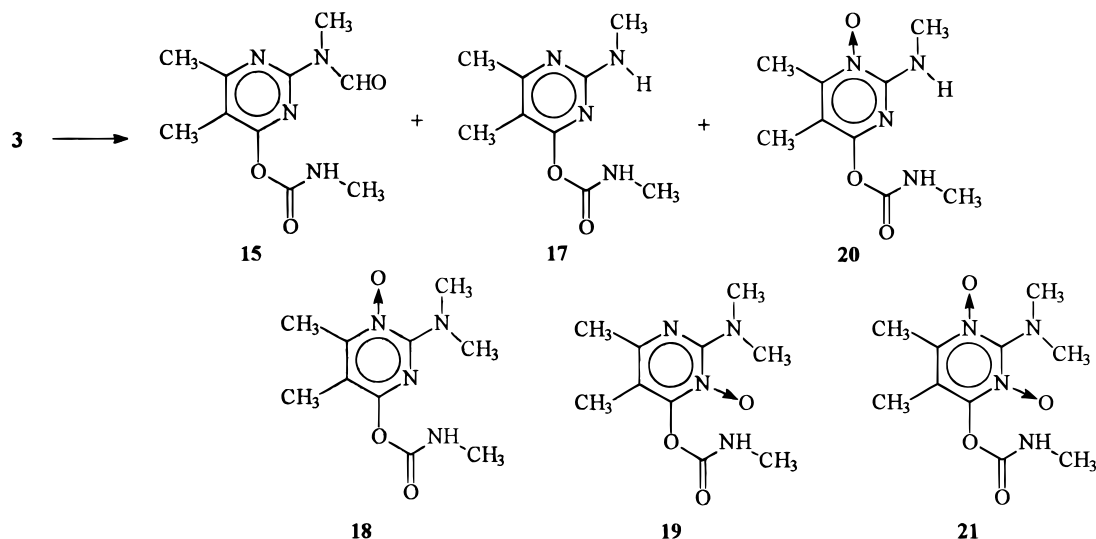


**Figure 4.** Products obtained by the biomimetic oxidation of **3**.

of 1,3-*N*-oxides was not detected in these reactions. Although N-oxidations cannot be affected by $H_2O_2$, a considerable amount of 1,3-*N*-oxide was identified in $H_2O_2$/Fe(TF$_{20}$PP)-mediated reactions. This unexpected reaction is related to the catalytic activity of the Fe(TF$_{20}$PP) metalloporphyrin catalyst and can be used for the preparation of pyrimidine 1,3-*N*-oxides.

**Comparison to Knowledge-Based Predictions.** Knowledge-based metabolic information systems were recognized as useful tools for the analysis of metabolic data. In addition to Metabolite (Metabolite, 1997), the complete metabolism information system of MDL used for metabolite data management prediction of metabolic pathways is also possible. MetabolExpert, a unique knowledge-based expert system for the metabolite prediction of drugs, pesticides, and xenobiotics, can be used at the initial stage of metabolic research (Darvas, 1988). Maps of metabolites obtained by this program could help in metabolite searching and interpretation of metabolite profiles. Testing our chemical model system, the oxidative metabolites of **1**−**3** were predicted by MetabolExpert implemented to the Pallas package (Pallas, 1996). Predicted metabolites of **1** involved 3-OH (**9**), 4-OH and 6-OH derivatives, and also a derivative demethylated at the carbamate nitrogen. The formation of **9** is in accordance with in vivo data; other hydroxylated products were isolated only in vitro. In contrast to knowledge-based predictions, demethylation at the carbamate nitrogen was not detected either in vivo or in biomimetic oxidations. Furthermore, the corresponding *N*-hydroxycarbamate (**6**) was not predicted by MetabolExpert; however, it was identified as a major oxidation product both in vivo and in model systems.

2-OH, 4-OH, 6-OH, and 7-OH analogues, as well as 3,4-, 5,6-, and 7,8-epoxides, were predicted to be the metabolites of **2**. 2- and 4-naphthols were also detected in biological systems. Epoxides were expected to form corresponding diols in the next stage of metabolism. Although the chemical model showed only limited performance on aromatic hydroxylation, a mixture of these diols could also be isolated from biomimetic oxidations. This is in accordance with the formation of the 5,6-dihydroxy metabolite observed in vivo. Predicted demethylation of the *N*-methylcarbamate moiety is in contrast to in vivo data; the nonpredicted in vivo hydroxylation at this *N*-methyl group, however, was reproduced by the biomimetic system.

Oxidative metabolites of **3** were predicted to be 5- and 6-hydroxymethyl analogues and *N*-oxides formed at N-1 and N-3 atoms of the pyrimidine ring and also at the carbamate nitrogen. N-oxidation at pyrimidine nitrogens was observed in catalytic oxidations, but the in vivo formation of these metabolites have not been confirmed yet. Oxidative transformation at the carbamate nitrogen, however, was detected in vitro. Although the formation of the previously described N-demethylated carbamate was predicted, again demethylation of the dimethylamino moiety was not assigned as a major metabolic pathway. It should be noted, however, that the latter was identified as the most important oxidative transformation in vivo, which was also detected as the major site of oxidation in biomimetic reactions.

**Conclusions.** A suitable chemical model of the CP450-catalyzed oxidative metabolism of carbamate insecticides was presented. Results obtained by the application of the biomimetic catalyst Fe(TF$_{20}$PP) revealed that in addition to the identification of metaboli-

cally susceptible functional groups, this system mimics the action of insect CP450s on carbamate insecticides. From a comparison of our results to knowledge-based predictions, it is apparent that our methodology can be considered as an equally useful tool for predicting oxidative metabolites and, furthermore, permits the modeling of in vivo metabolic profiles semiquantitatively.

## ABBREVIATIONS USED

mCPBA, *m*-chloroperbenzoic acid; [Fe(TF$_{20}$PP)], *meso*-tetrakis(pentafluorophenyl)porphyrin iron(III) chloride; [Fe(TCl$_8$PP)], *meso*-tetrakis(2,6-dichlorophenyl)porphyrin iron(III) chloride.

## ACKNOWLEDGMENT

## LITERATURE CITED

Andersen, K. E.; Begtrup, M.; Chorghade, M. S.; Lee, E. C.; Lau, J.; Lundt, B. F.; Petersen, H.; Sorensen, P. O.; Thogersen, H. The synthesis of novel GABA uptake inhibitors. Part 2. Synthesis of 5-hydroxytiagabine, a human metabolite of the GABA reuptake inhibitor Tiagabine. *Tetrahedron* **1994**, *50*, 8699−8710.

Artaud, I.; Ben-Aziza, K.; Mansuy, D. Iron Porphyrin-Catalyzed Oxidation of 1,2 Dimethoxyarenes: A Discussion of the Different Reactions Involved in the Competition between the Formation of Methoxyquinones or Muconic Dimethyl Esters. *J. Org. Chem.* **1993**, *58*, 3373−3380.

Balba, M. H.; Singer, M. S.; Slade, M.; Casida, J. E. Synthesis of Possible Metabolites of Methylcarbamate Insecticide Chemicals. Substituted Aryl-N-hydroxymethylcarbamates. *J. Agric. Food Chem.* **1968**, *16*, 821−825.

Benezet, H. J.; Matsumura, F. Factors influencing the metabolism of Mexacarbate by microorganisms. *J. Agric. Food Chem.* **1974**, *22*, 427−430.

Brown, D. J. *The Pyrimidines. The Chemistry of Heterocyclic Compounds*; Wiley-Interscience: New York, 1994; Vol. 52, pp 542−545.

Chorghade, M. S.; Dezaro, D. A.; Hill, D. R.; Lee, E. C.; Pariza, R. J.; Andersen, J. V.; Hansen, K. T.; Dolphin, D. H. Metalloprophyrins as chemical mimics of cytochrome P-450 systems. *Bioorg. Med. Chem. Lett.* **1994**, *4*, 2867−2870.

Chorghade, M. S.; Dolphin, D.; Dupre, D.; Hill, D. R.; Lee, F. C.; Wijesekera, T. P. Improved Protocol for the Synthesis and Halogenation of Sterically Hindered Metalloporphyrins. *Synthesis* **1996**, 1320−1324.

Darvas, F. Predicting Metabolic Pathways by Logic Programming. *J. Mol. Graph.* **1988**, *6*, 80−87.

Dolphin, D.; Taylor, T. G.; Xie, L. Y. Polyhaloporphyrins: Unusal Ligands for Metals and Metal-Catalyzed Oxidations. *Acc. Chem. Res.* **1997**, *30*, 251−259.

Dorough, H. W.; Casida, J. E. Nature of Certain Carbamate Metabolites of the Insecticide Sevin. *J. Agric. Food Chem.* **1964**, *12*, 294−304.

Eldefrawi, M. E.; Miskus, R.; Sutcher, V. Methylenedioxyphenyl derivatives as synergists for carbamate insecticides on susceptible, DDT- and parathion-resistant houseflies. *J. Econ. Entomol.* **1960**, *53*, 231−234.

Feyereisen, R. Molecular Biology of Insecticide Resistance. *Toxicol. Lett.* **1995**, *82/83*, 83−90.

Fuju, K.; Ichikawa, K.; Node, M.; Fujita, E. Hard Acid and Soft Nucleophil System. New Efficient Method for Removal of Benzyl Protecting Group. *J. Org. Chem.* **1979**, *44*, 1661−1664.

Hassal, K. A. *The Biochemistry and Uses of Pesticides*; VCH: Weinheim, 1990; p 124.

Hodgson, E.; Rose, R. L.; Goh, D. K. S.; Rock, G. C.; Roe, R. M. Insect cytochrome P-450: metabolism and resistance to insecticides. *Biochem. Soc. Trans.* **1993**, *21*, 1060−1065.

Johnstone, R. A. W.; Nunes, P. G.; Pereira, M. M.; Gonsalves, M. A. R. Improved Synthesis of 5,10,15,20-tetrakisaryl and tetrakisalkyl porphyrins. *Heterocycles* **1996**, *43*, 1423−1437.

Jung, M. E.; Lyster, M. A. Quantitative Dealkylation of Alkyl Ethers via Treatment with Trimethylsilyl Iodide. A New Method for Ether Hydrolyzis. *J. Org. Chem.* **1977**, *42*, 3761−3763.

Keserü, G. M. Cytochrome P450 Catalyzed Insecticide Metabolism. Chemical and Theoretical Models. *Sci. Prog.* **1998**, *81*, 245−272.

Keserü, G. M.; Kolossváry, I.; Bertók, B. Cytochrome P-450 catalysed insecticide metabolism. Prediction of regio- and stereoselectivity in the primer metabolism of carbofuran: a theoretical study. *J. Am. Chem. Soc.* **1997**, *119*, 5127−5131.

Keserü, G. M.; Balogh, T.; Bokotey, S.; Árvai, G.; Bertók, B. Metalloporphyrin Catalyzed Biomimetic Oxidation of Aryl Methyl Ethers. *Tetrahedron* **1999**, in press.

Knaak, J. B.; Tallant, M. J.; Bartley, W. J.; Sullivan, L. J. The Metabolism of Carbaryl in the Rat, Guinea Pig, and Man. *J. Agric. Food Chem.* **1965**, *13*, 537−543.

Kuhr, R. J.; Dorough, H. W. *Carbamate Insecticides: Chemistry, Biochemistry and Toxicology*; CRC Press: Cleveland, OH, 1976; Chapter 6.

Lamoureux, G. L.; Rusness, D. G. Status and Future of Synergists in Resistance Management. In *8th IUPAC Congress of Pesticides*; Ragsdale, N. N., Kearney, P. C., Plimmer, J. R., Eds.; ACS Conference Proceedings Series; American Chemical Society: Washington, DC, 1995; pp 350−366.

MacFaul, P. A.; Arends, I. W. C.; Ingold, K. U.; Wayner, D. M. Oxygen Activation by Metal Complexes and Alkyl Hydroperoxides. Application ol Mechanistic Probes to Explore the Role of Alkyloxy Radicals in Alkane Functionalization. *J. Chem. Soc., Perkin Trans. 2* **1997**, 135−144.

Metabolite, MDL Information Systems, San Leandro, CA, 1997.

Metcalf, R. C.; Borck, K.; El-Aziz Munoz, S. A.; Casillo, C. C. Metabolism of 2,2-dimethyl-2,3-dihydrobenzofuranyl-7-*N*-methylcarbamate (Furadan) in Plants, Insects and Mammals. *J. Agric. Food Chem.* **1968**, *16*, 300−311.

Montanari, F., Casella, L, Eds. *Metalloporphyrins Catalysed Oxidations*; Kluwer Academic Press: Dordrecht, The Netherlands, 1994.

Mulin, C. A., Scott, J. G., Eds. *Molecular Mechanism of Insecticide Resistance*; ACS Symposium Series 505; American Chemical Society: Washington, DC, 1992.

Nagatsu, Y.; Higuchi, T.; Hirobe, M. Application of chemical P-450 model systems to drug metabolism III. Metabolism of 3-isobutyryl-2-isopropylpyrazolo[1,5-a]pyridine. *Chem. Pharm. Bull.* **1993**, *38*, 400−403.

Pallas for Windows 2.0, Metabolic Prediction Module: Metabol-Expert 10.0, CompuDrug Chemistry Ltd., USA, 1996.

*The Pesticide Manual*, 11th ed.; British Crop Protection Council: Farnham, UK, 1997.

Traylor, P. S.; Dolphin, D.; Traylor, T. G. Sterically protected hemins with electronegative substituents: efficient catalysts for hydroxylation and epoxidation. *J. Chem. Soc., Chem. Commun.* **1984**, 279−280.

Volmer, D. A. Investigation of photochemical behavior of pesticides in a photolysis reactor coupled on-line with a liquid chromatography-electrospray ionization tandem mass spectrometry system. Application to trace and confirmatory analyses in food samples. *J Chromatogr. A* **1998**, *794*, 129−146.